Structural and magnetic properties of $Co_{1-x}Fe_xSr_2YCu_2O_{7+\delta}$ compounds

Shiva Kumar Singh,[1,2,a)] Praveen Kumar,[1] M. Husain,[2] Hari Kishan,[1] and V. P. S. Awana[1]
[1]*National Physical Laboratory, CSIR, New Delhi 110012, India*
[2]*Department of Physics, Jamia Millia Islamia University, New Delhi 110025, India*

(Received 13 November 2009; accepted 26 January 2010; published online 23 March 2010)

Here we study the structural and magnetic properties of the $Co_{1-x}Fe_xSr_2YCu_2O_{7+\delta}$ compound ($0 \leq x \leq 1$). X-ray diffraction patterns and simulated data obtained from Rietveld refinement of the same indicate that the iron ion replacement in $Co_{1-x}Fe_xSr_2YCu_2O_{7+\delta}$ induces a change in crystal structure. The orthorhombic *Ima*2 space group structure of Co-1212 changes to tetragonal *P*4/*mmm* with increasing Fe ($x \geq 0.5$) ion. The XPS studies reveal that both Co and Fe ions are in mixed states of 3+/4+ for the former and 2+/3+ in case of later. The magnetization with temperature follows Curie–Weiss behavior, in the range of 150–300 K and short magnetic correlations/spin glasslike features below 150 K. The observed magnetic behavior is due to competition of antiferro/ferromagnetic exchange interaction of Co^{3+} [intermediate spin (IS)]-O–Co^{3+} (IS)/Co^{4+} [low spin (LS)] and Fe^{3+} [high spin (HS)]-O–Fe^{2+} (LS)/Fe^{3+} (HS)/Co^{3+} (IS)/Co^{4+} (LS) states. Although none of the studied as synthesized samples in $Co_{1-x}Fe_xSr_2YCu_2O_{7+\delta}$ are superconducting, the interesting structural changes in terms of their crystallization space groups and the weak magnetism highlights the rich solid state chemistry of this class of materials. © *2010 American Institute of Physics*. [doi:10.1063/1.3327452]

I. INTRODUCTION

Charge transport and high temperature superconductivity (HTSC) is believed to reside in the CuO_2 planes of all known HTSC cuprates, except that $CuO_{1+\delta}$ chains have been reported to participate in the *b*-axis transport of $YBa_2Cu_3O_{7-\delta}$.[1] In $YBa_2Cu_3O_{7-\delta}$ ($CuBa_2YCu_2O_{7-\delta}$, Cu-1212) there are two different Cu sites, namely, Cu1 and Cu2. Cu1 resides in $CuO_{1+\delta}$ chains and Cu2 in superconducting CuO_2 planes. Even at macroscopic level, any contravene in integral CuO_2 stacks, affects superconductivity drastically.[2,3] The $CuO_{1+\delta}$ chain acts as a charge reservoir and provides the mobile carriers to superconducting CuO_2 planes.

A variety of high-T_c superconductive compounds are related with M-1212 structure. The M-1212 structure tolerates a wide range of single-element constituents such as Cu, Co, Fe, Nb, Ta, Ru, Hg, Tl, Al, Ga, and various cation mixtures as M.[4–8] Some of the M-1212 phases are well-established superconductors (viz., Cu-1212), whereas some of them are nonsuperconducting yet (viz., Nb/Al-1212). The M-1212 phases with M=Ga, Al, and Co, particularly, have attracted considerable interest as potential superconducting candidates due to the complicated structure of their $MO_{1\pm\delta}$ charge reservoirs.[4–8] In the charge reservoir, the M cations are tetrahedrally coordinated by oxygen atoms to form chains of corner-sharing MO_4 tetrahedra that run diagonally relative to the perovskite base. Further, it has been reported that the MO_4 tetrahedra are arranged into two kinds of chain, L (left) and R (right) in which the tetrahedra rotate in different ways.[7–9] The M-1212 phases with M=Fe, Nb, Tl, and Ru has a tendency to form MO_6 octahedra, which have similar rotation in each unit cell resulting in tetragonal structure. The oxygen stoichiometry plays a crucial role in determining superconductivity and structure of these compounds. Changes in the concentration of vacancies due to oxygen may lead to structural and electronic phase transitions. The polyhedra formation of charge reservoir blocks ($MO_{4/6}$) depends upon the oxygen intake ability of the M. It has been reported that in Fe-1212, Fe forms FeO_6 octrahedra in oxygenated Fe-1212 system. However, after annealing in nitrogen atmosphere, it loses oxygen and is left with FeO_4 tetrahedra[10] resulting tetragonal to orthorhombic structure of Fe-1212. The Co-1212 ($CoSr_2YCu_2O_{7+\delta}$) phase has orthorhombic structure with CoO_4 tetrahedra. However the Co-1212 phase with Ba ion on Sr ion site ($Cu_{1-x}Co_xBa_2YCu_2O_{7+\delta}$, x=0.84 composition) was reported to crystallize in tetragonal *P*4/*mmm* space group.[11] This suggests that besides M, other constituents are also the deciding factor in the structure formation of cuprates. M=Ga and Co are made superconducting after annealing in ultrahigh pressure oxygen. The structural changes and the reason behind superconductivity are not revealed yet. There may be ultrapressure oxygen introduces itself in reservoir blocks and causes change from tetrahedra (Co/GaO_4) to octahedra (Co/GaO_6) resulting orthorhombic-tetragonal: O-T transformation. We have taken Co (which prefers CoO_4 tetrahedra) and Fe (which prefers FeO_6 octahedra) formation in reservoir blocks to investigate structural changes. Also, cobalt and iron both have ferromagnetic nature, but the magnetic behavior of their pervoskite compounds is quite different from each other. The distinct magnetic feature in these pervoskites is due to the various spin states of Co and Fe ions. There are reports on pervoskite cobaltites that spin states of cobalt can be low spin (LS) and mixture of intermediate spin (IS) and/or LS for tetravalent and trivalent cobalt ions, respectively.[12–16] Actually, the spin state of Co^{3+} is controversial: the high spin (HS) state (HS,

a)Author to whom correspondence should be addressed. Electronic mail: singhsk@mail.nplindia.ernet.in. Tel.: 91-11-45609210. FAX: 91-11-45609310.

t_{2g}^4 e_g^2), IS state (IS, t_{2g}^5 e_g^1), and a superposition of HS and LS spin states are all proposed[16–18] in cobaltites. Here, the magnetic nature of $Co_{1-x}Fe_x$-1212 whose structure belongs to HTSC cuprate family, can be explained by Goodenough–Kanamori rule of superexchange[19–21] as in cobaltites. Here we are revealing the structural changes and magnetic properties and effect of these properties on each other in charge transport.

II. EXPERIMENTAL DETAILS

The samples are synthesized in air by solid-state reaction route. The stoichiometric mixture of Co_3O_4, Fe_3O_4, $SrCO_3$, Y_2O_3, and CuO are ground thoroughly, calcined at 900 °C for 12 h, and then presintered at 950 and 980 °C for 15 h with intermediate grindings. Finally, the powders are palletized and sintered at 1000 °C for 15 h in air. The phase formation is checked for each sample with powder diffractometer, Rigaku (Cu $K\alpha$ radiation) at room temperature. The phase purity and lattice parameter refining are done by Reitveld refinement program (Fullprof version).The magnetization measurements are carried out on Quantum Design superconducting quantum interference device magnetometer MPMS-XL. The samples have been characterized by x-ray photoelectron spectroscopy (XPS), Perkin Elmer (PHI Model 1257), working at a base pressure of 5×10^{-10} torr. The chamber is equipped with a dual anode Mg $K\alpha$ (1253.6 eV) and Al $K\alpha$ (1486.6 eV) x-ray sources and a high-resolution hemispherical electron energy analyzer. We have used Mg $K\alpha$ x-ray source for our analysis. The calibration of the binding energy scale has done with the C (1s) line at 284.6 eV. The core level spectra of Co and Fe have been deconvoluted in to the Gaussian components.

III. RESULTS AND DISCUSSION

All the samples are crystallized in single phase which is confirmed from the Rietveld analysis of powder x-ray diffraction (XRD) pattern. The compositions with $x<0.5$ are fitted in orthorhombic *Ima*2 space group (Fig. 1), whereas compositions with $x\geq0.5$ are fitted in tetragonal $P4/mmm$ space group (Fig. 2). The change in space group from *Ima*2 to $P4/mmm$ appears in the XRD pattern. The *020* peak associated with main *002* peak of *Ima*2 space group disappears and single *103* peak of $P4/mmm$ space group appears with increasing Fe ion concentration [Fig. 3(a)]. This clearly suggests the absence of *b*-axis contribution, i.e., the L and R chains, due to the rotation of CoO_4 tetrahedra in different direction within one unit cell, are disappearing. The same can be seen with 631 peak of *Ima*2 space group [Fig. 3(b)]. The lattice parameters obtained from Rietveld refinement of the XRD shows that as Fe concentration increases on Co site there is a variable change in the lattice parameters [Table I]. The *a*-parameter increases from x=0.0 to x=0.3 composition. The *b*- and *c*-parameter almost remained constant from x=0.0 to x=0.3 composition. However, for x=0.4, there is a decrease in all these parameters. It can be interpreted as follows: considering the ionic radii of Co ions {Co^{3+} (CN=6) 0.545 Å LS, 0.56 Å IS, 0.61 Å HS; Co^{4+} 0.40 Å, (CN=4), 0.53 Å HS (CN=6)}, Fe ions {Fe^{2+} 0.61 Å LS (CN=6), Fe^{3+}

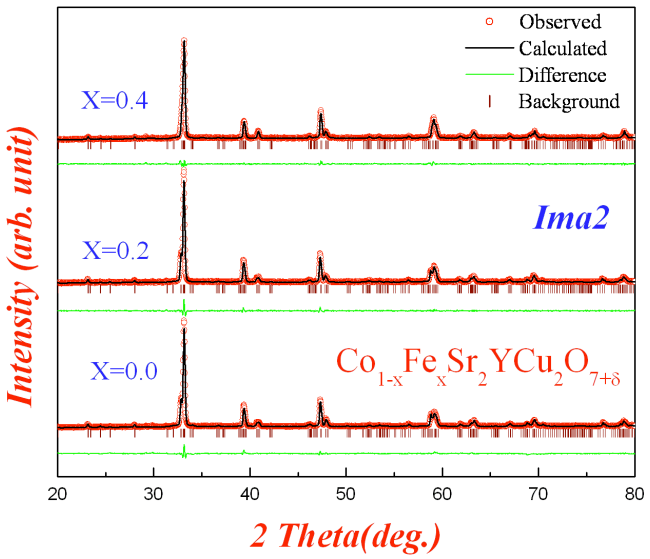

FIG. 1. (Color online) Reitveld fitted XRD pattern of $Co_{1-x}Fe_xSr_2YCu_2O_{7+\delta}$ (x=0.0, 0.2, and 0.4) samples with space group *Ima*2.

0.49 Å (CN=4), 0.58 Å (CN=5), 0.55 Å LS, 0.645 Å HS (CN=6); Fe^{4+} 0.585 Å (CN=6)}, and Cu ions {Cu^{2+} 0.57 Å (CN=4), 0.64 Å (CN=5), 0.73 Å (CN=6); Cu^{3+} 0.54 Å LS (CN=6)}.[22] The change in lattice parameters from x=0.0 to 0.4 can be explained as: Co ions are in mixed 3+(CN=6,IS) and 4+(CN=4) (Ref. 23) states are being replaced by $Fe^{2+/3+}$ ions. This is also evident from the XPS and M-T measurements of these compounds (to be discussed latter). The decrease in parameters for x=0.4 indicates toward origination of change in space group orthorhombic (*Ima*2)-tetragonal ($P4/mmm$): (O-T). This means that the $FeO_{4/6}$ tetra/octahedra are not as tilted as pure CoO_4 tetrahedra in x=0.0, but getting more similar rotation in consecutive unit cells leading decrease in lattice parameters. For compositions $x\geq0.5$ the lattice parameters decreases with increasing iron concentration. There may be two reasons of this decrease, (1) The minor decrease in *a*- and *b*-parameters (in

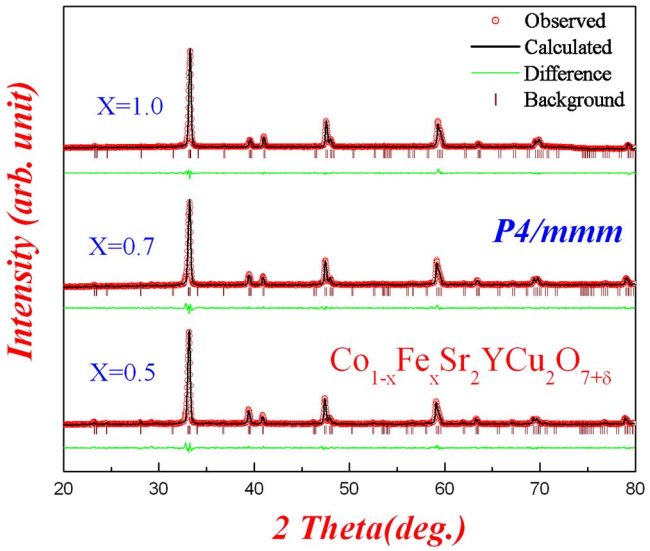

FIG. 2. (Color online) Reitveld fitted XRD pattern of $Co_{1-x}Fe_xSr_2YCu_2O_{7+\delta}$ (x=0.5, 0.7, and 1.0) samples with space group $P4/mmm$.

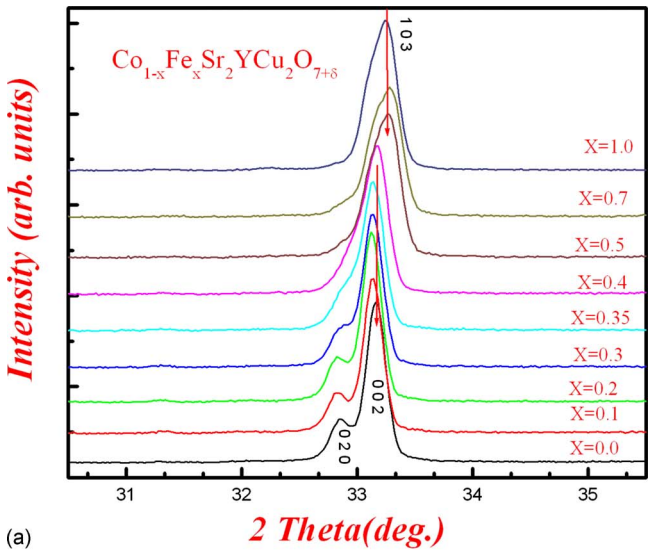

(a)

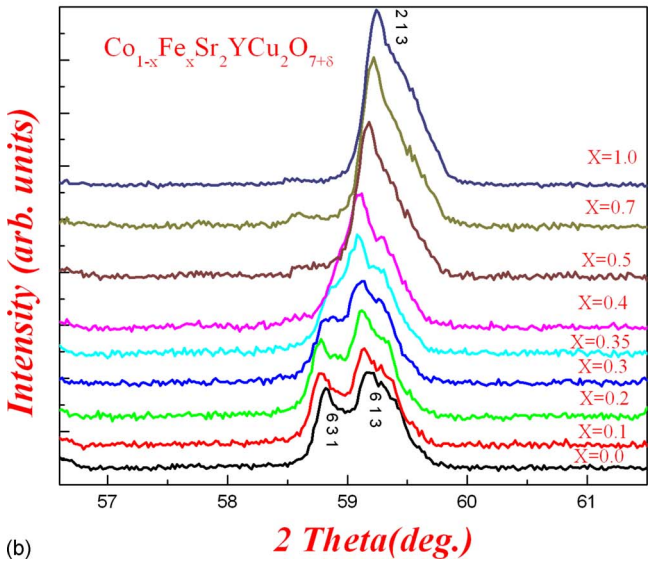

(b)

FIG. 3. (Color online) (a) X-ray pattern of main 002 peak of *Ima*2 and 103 peak of *P*4/*mmm* space group. The change in space group from *Ima*2 to *P*4/*mmm* can be seen as the 020 peak associated with main 002 peak of *Ima*2 disappearing and single 103 peak of *P*4/*mmm* is appearing with increasing Fe ion concentration. The arrows shows shift toward lower angle in 2θ as volume increases in ($x \leq 0.4$) in *Ima*2 space group, and toward higher angle in 2θ as volume decreases in ($0.5 \leq x \leq 1.0$) in *P*4/*mmm* space group. (b) X-ray pattern of main *613* peak of *Ima*2 and *213* peak of *P*4/*mmm*. The change in space group from *Ima*2 to *P*4/*mmm* can be seen as the *631* peak associated with main 613 peak of *Ima*2 disappearing and single 213 peak of *P*4/*mmm* space group is appearing with increasing Fe ion concentration. The shift toward higher angle in 2θ is more prominent with 213 peak.

respect to concentration [see Table I]) is attributed to the same O-T (*Ima*2-*P*4/*mmm*) transition. As with decrease in Co concentration the CoO_4 tetrahedra density is also decreasing so there are more tetra/octahedrons rotated in centrosymmetrical fashion, resulting shrinkage of *a*- and *b*-parameters. (2) The decrease in *c*-parameter (minor) can be attributed to the intermixing of Cu ions and Fe ions at Cu2 and Fe1 (Cu1) sites. There are reports that the Fe ion replaces Cu ion at Cu2 site up to 22%–47%.[2,3] Fe ions in all possible ionic (2+/3+/4+) and coordination states ($FeO_{4/6}$ tetra/octahedra) have larger ionic radii than Co ions so the lattice parameters should increase. Whereas Fe ion at Cu2 site, i.e., in CN=5 have lower ionic radii than Cu ion in the same coordination but in different ionic state. However Cu ions replacing Co/Fe ions at Fe1(Cu1) site have larger ionic radii resulting increase in *c*-parameter. However, this change is lower than former and therefore, there is overall minor decrease in *c*-parameter. Thus it seems that at higher iron concentration Fe ion is replacing Cu ion at Cu2 site. Though x ray cannot resolve issue of intermixing of Fe at Cu1 and Cu2 sites and exact percentage and only the neutron diffraction and Mossbauer spectroscopy can resolve.[2,3,24] However, the same is clearly indicates toward intermixing of Cu ions and Fe ions at Cu2 and Fe1(Cu1) sites. The ambiguity in intermixing of Cu ions and Fe ions at Cu2 and Fe1(Cu1) sites in XRD pattern of studied samples can be attributed to almost equal structure factors of iron and copper.

To find out the oxidation state of Co and Fe, the XPS study have been carried out for two samples x=0.0 and 0.7 ($CoSr_2YCu_2O_{7+\delta}$ and $Co_{0.3}Fe_{0.7}Sr_2YCu_2O_{7+\delta}$). The Co (2*p*) and Fe (2*p*) core level spectra have been deconvoluted into the different Gaussian component to find out the contribution of different ionic states. The deconvoluted Co (2*p*) core level spectra for samples x=0.0 and 0.7 are shown in Fig. 4(a). Comparing to the spectrum of x=0.0, the binding energy of two main component of Co ($2p_{3/2}$ and Co $2p_{1/2}$), in the spectrum for the sample x=0.7, shifts toward higher binding energy. We have observed peak broadening in the x=0.7 in comparison with x=0.0. Deconvolution of Co (2*p*) core level spectra shows the presence of Co^{3+} and Co^{4+} with a satellite peak, at the binding energy of 779.45 eV and 781.85 eV for Co ($2p_{3/2}$) and 795.00 and 797.05 eV for Co ($2p_{1/2}$), respectively, in both compositions. The similar kinds of results have also been reported in literature regarding concentration and binding energy of $Co^{3+/4+}$.[23,25] Curve shows the domination of Co^{3+} state over Co^{4+} state for x=0.0 sample, but for

TABLE I. Rietveld refined lattice parameters and unit cell volume $Co_{1-x}Fe_xSr_2YCu_2O_{7+\delta}$ ($0.0 \leq x \leq 1.0$) compounds.

$Co_{1-x}Fe_x$-1212	x=0.0	x=0.1	x=0.2	x=0.3	x=0.4	x=0.5	x=0.7	x=1.0
a (Å)	22.78(2)	22.79(7)	22.80(6)	22.81(2)	22.79(1)	3.83(3)	3.82(9)	3.82(1)
b (Å)	5.45(1)	5.45(3)	5.45(2)	5.44(8)	5.43(7)	3.83(3)	3.82(9)	3.82(1)
c (Å)	5.40(9)	5.41(0)	5.41(1)	5.41(2)	5.41(3)	11.38(8)	11.37(8)	11.36(1)
V (Å^3)	671.74(8)	672.52(4)	672.80(3)	672.63(0)	670.73(7)	167.29(5)	166.79(1)	165.88(1)
R_p	2.11	2.52	2.48	2.48	2.54	2.74	2.92	2.45
R_{wp}	2.85	3.42	3.37	3.23	3.30	3.76	3.98	3.34
Chi^2	2.35	3.18	3.21	2.66	2.89	3.72	3.84	2.20

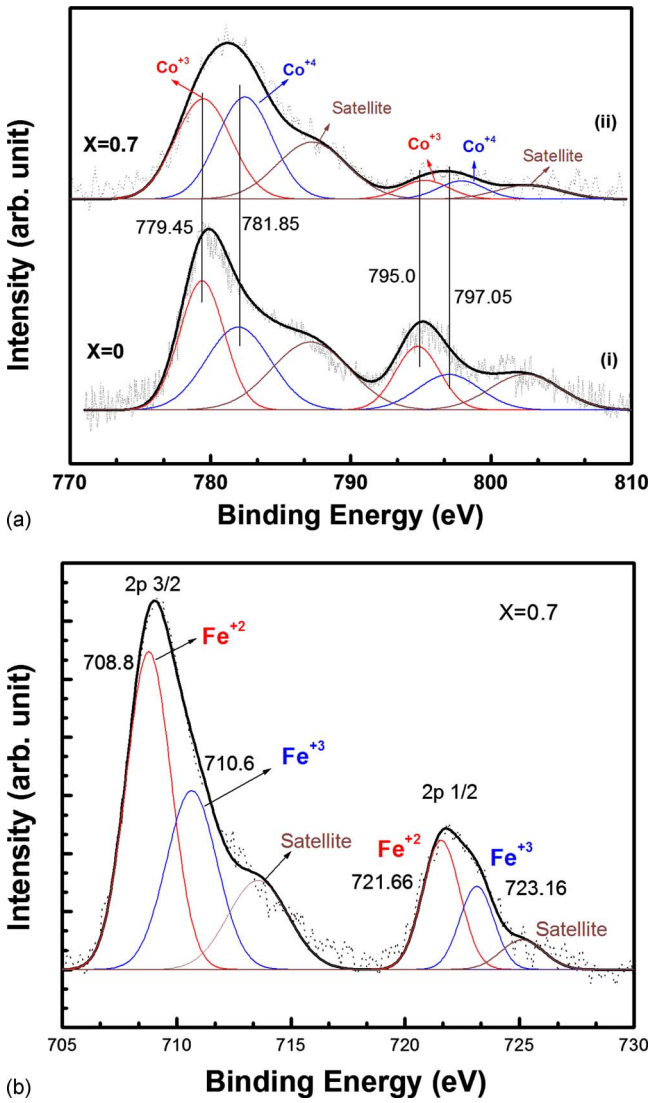

FIG. 4. (Color online) (a) The Co $2p$ XPS spectra for the sample $x=0.1$ and 0.7. (b) The Fe $2p$ XPS spectra for the sample x=0.7. The dashed line represents the experimental curve and the solid line represents the resultant of fitted curve.

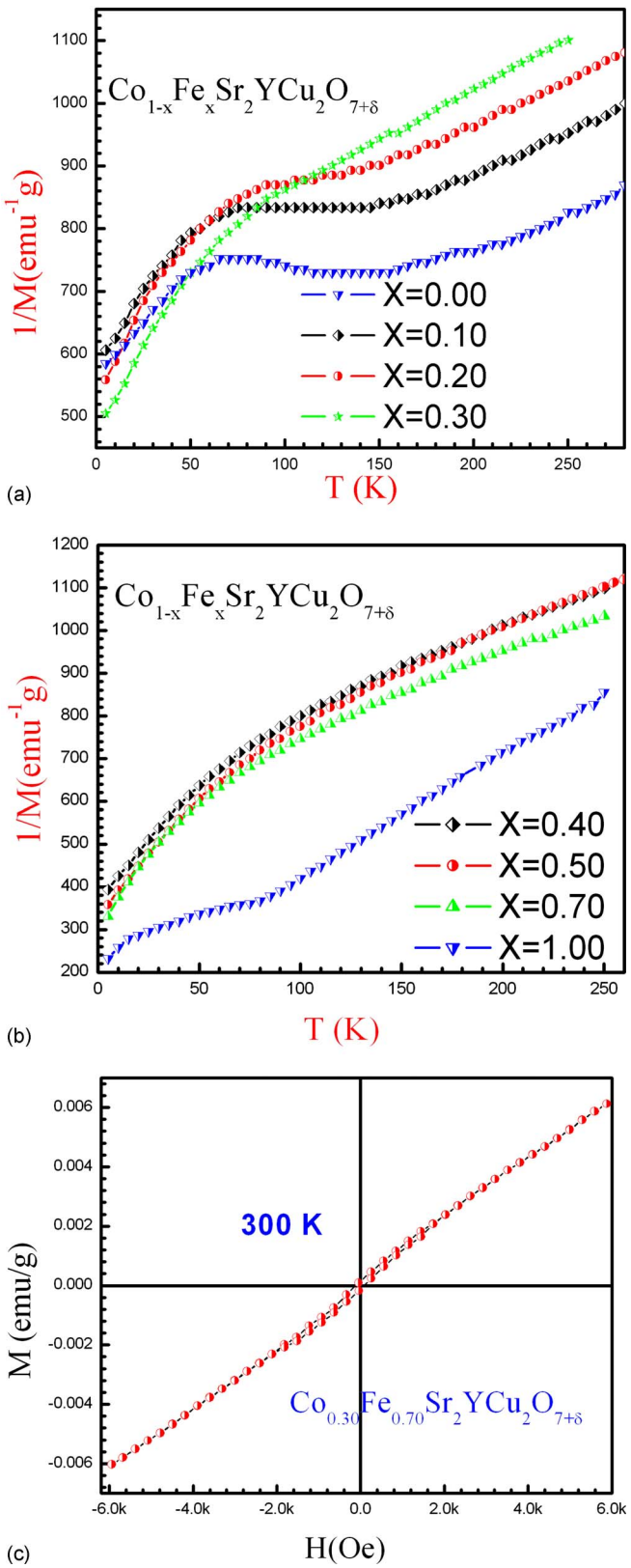

FIG. 5. (Color online) (a) 1/M vs T (ZFC) of $Co_{1-x}Fe_xSr_2YCu_2O_{7+\delta}$ x=0.0, 0.1, 0.2, and 0.3 samples. (b) 1/M vs T (ZFC) of $Co_{1-x}Fe_xSr_2YCu_2O_{7+\delta}$ x=0.4, 0.5, 0.7, and 1.0 samples. (c) M-H of x=0.7 sample at room temperature.

x=0.7 both states are almost equal. This increase in Co^{4+} ions concentration can be attributed due to the presence of major fraction of Fe in 2+ state in x=0.7. In x=0.7, composition there is slight increase in binding energy of both Co^{3+} and Co^{4+} component than that in x=0.0 composition. Fe ions are in mixed 2+/3+ state in x=0.7 composition, as shown in Fig. 4(b). The Fe^{2+} ions are in higher concentration than Fe^{3+} ions. The Fe $2p_{3/2}$ main peak maximum of the Fe^{2+} component has a binding energy of 708.8 eV, while that of the Fe^{3+} components is 710.6 eV as in γ-Fe_2O_3 reported in Ref. 26. In γ-Fe_2O_3 iron ions coordinate both tetra and octahedrally with oxygen the same is in the studied samples. On the other hand, the $2p1/2$ main peak has a binding energy of 721.66 and 723.16 eV for Fe^{2+} and Fe^{3+} ions, respectively. The ionic composition of Co and Fe, thus found by XPS study are supportive to magnetic behavior of studied samples.

The magnetization measurement (M-T) [zero field cooled (ZFC) and field cooled] for all the samples is done in magnetic field of strength 100 Oe. The magnetic behavior in x=0.0, 0.1, 0.2, and to some extent in 0.3 is like Curie–Weiss in the temperature range of 150–300 K [Fig. 5(a)]. This is an intermediate behavior of antiferromagnetic and ferromagnetic ordering. Below 150 K, spin glass (SG) or canted fer-

romagnetism type broad down-turn is observed in magnetization measurement of x=0.0, 0.1, and 0.2, which is dominated by the paramagnetic contribution below 50 K.[27] The magnetization behavior of x=0.4, 0.5, and 0.7 is slightly different from the x=0.0, 0.1, and 0.2. These concentrations show intermediate behavior of antiferro/ferromagnetic nature in the temperature range of 100–300 K in which ferromagnetic is dominating, as Fe ion concentration is increasing [Figs. 5(b) and 5(c)]. However, below 50 K, the behavior is same as that in lower concentrations. The x=1.0 composition is more prominent with ferromagnetic nature in which the paramagnetic to ferromagnetic transition occurs around 80 K in ZFC M-T plot. In $Co_{1-x}Fe_x$-1212, the presence of the Co^{3+}, Co^{4+}, Fe^{2+}, and Fe^{3+} ions make the magnetic behavior more complicated. Since LS Co^{3+} ions carry no magnetic moment[28] and HS Co^{3+} ions have greater ionic radii that are contradictory to Rietveld refined parameters so we can say Co^{3+} ions in IS state. However the magnetic properties in the temperature range of 50–300 K can be interpreted by Goodenough–Kanamori rule of superexchange, which applies to interatomic spin-spin interactions between two atoms, each carrying a net spin, that are mediated by virtual electron transfers between the atoms (superexchange). This rule states that superexchange interactions are antiferromagnetic where the virtual electron transfer is between overlapping orbitals that are each half-filled, but they are ferromagnetic where the virtual electron transfer is from a half-filled to an empty orbital or from a filled to a half-filled orbital. In the lower concentration range (≤0.2), the weak antiferromagnetic behavior (300–50 K) can be explained by Co^{3+} (IS)-O–Co^{3+} (IS) and Co^{3+} (IS)-O–Co^{4+} (LS) electron exchange as in cobaltites.[29,30] Actually, this rule cannot directly tell whether the exchange interactions through Co^{3+} (IS)-O–Co^{3+} (IS) and Co^{3+} (IS)-O–Co^{4+} (LS) (partially filled-partially filled and partially filled-empty e_g orbitals) are ferromagnetic or antiferromagnetic because the sign of this interaction depends on the relative orientation of unoccupied/occupied e_g orbitals. Although the relative orientation information of the orbitals in the present materials is not available but with the magnetic nature of studied samples and in the presence of variety of spins [Co^{3+} (IS), Co^{4+} (LS), Fe^{2+} (LS), and Fe^{3+} (HS)], we could propose that antiferromagnetic exchange and ferromagnetic exchange are competing here in which antiferromagnetic exchange is dominating. This results in weak antiferromagnetism and/or spin glasslike behavior since spins got frustrated with these competition. The magnetic behavior of compounds with higher Fe ion concentrations (0.4≤x≤1.0) can be explained by the same exchange interaction. Here the Fe^{3+} (HS)-O–Co^{3+} (IS)/Co^{4+} (LS) and Fe^{3+} (HS)-O–Fe^{2+} (LS) and/or Fe^{2+} (LS)-O–Cu^{3+} (LS) and Cu^{3+} (LS)-O–Co^{3+} (IS)/Co^{4+} (LS) (in case of intermixing of Cu ions and Fe ions at Cu2 and Fe1 (Cu1) sites, which infers from Rietveld refinement in compounds of higher Fe ion concentration) exchange interaction is being taken place. The ferromagnetic nature (ZFC) of x=1.0 also indicates about mixed state of $Fe^{2+/3+}$ ions since Fe^{3+} (HS)-O–Fe^{2+} (LS) exchange interaction is ferromagnetic. The same antiferromagnetic exchange and ferromagnetic exchange are in competition. However, here the ferromagnetic exchange is dominating and is more prominent in higher Fe ion concentrations resulting weak ferromagnetism. However the contribution of ferromagnetic Fe spins toward domination of ferromagnetic nature in higher Fe ion concentration compounds cannot be excluded completely. In the lower temperature range (<50 K), the frustration of spins due to these antiferro/ferromagnetic competition results in paramagnetic nature. The variation in moment is monotonic with the Fe concentration at 5 K and the same is nonmonotonic at 300 K and it can be explained as follows. The magnitude of magnetization decreases from x=0.0 to x=0.3 in higher temperature range this is due to Co^{3+} (IS) got replaced by Fe^{2+} (LS)/Fe^{3+} (HS). Since Fe^{2+} (LS) is in higher concentration and have lower magnetic moment than Co^{3+} (IS) {having higher number of unpaired electrons than Fe^{2+} (LS)}. The magnitude of magnetization remains almost equal for x =0.3, 0.4, and 0.5. However there is increase in the magnitude of magnetization from x=0.5 to x=1.0 and x=1.0 have slightly higher magnitude than that of the x=0.0 [Figs. 5(a), 5(b), and 6]. It is due as follows: (1) as we concluded that in higher Fe concentration samples, there is an increase in Co^{4+} (LS) and there may be intermixing of Fe and Cu ions at Cu1/Cu2 site. Thus replacement of Co^{3+} (IS) by Co^{4+} (LS)/Fe^{2+} (LS) results in decrease in magnitude; however it got compensated by an increase in magnitude by Co^{3+} (LS)/Fe^{3+} (HS) ions. Hence, there is a small increase in intermediate concentrations (0.3≤x≤0.7). (2) For x=1.0 Cu^{3+} (LS)/Fe^{3+} (HS) have higher magnetic moment than Co^{3+} (IS)/Co^{4+} (LS). In lower temperature (<50 K) range the paramagnetic ordering starts after weak antiferromagnetic/SG in lower x concentrations and after weak ferromagnetic ordering in higher x concentration range and hence is monotonic.

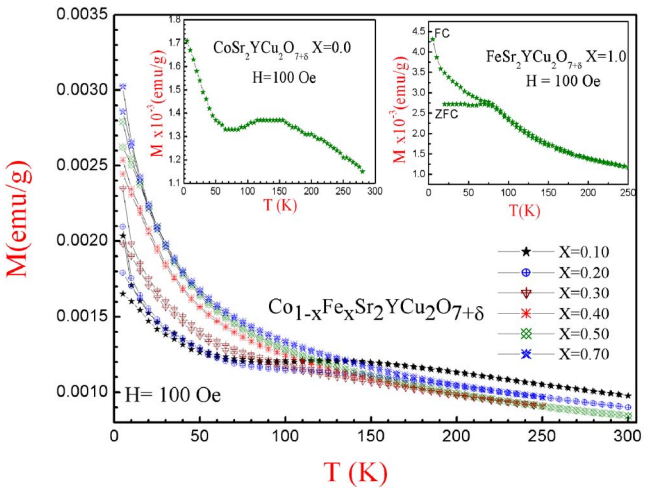

FIG. 6. (Color online) Magnetization vs temperature (M-T) behavior of $Co_{1-x}Fe_xSr_2YCu_2O_{7+\delta}$ (0.1≤x≤0.7); inset shows the (M-T) behavior of x=0.0 and 1.0.

IV. CONCLUSION

The studied compounds show that with increasing Fe concentration both structural and magnetic properties changes. The orthorhombic (*Ima*2 space group) structure of Co-1212 crystallizes in tetragonal *P*4/*mmm* of Fe-1212.

XPS study reveals that Co ions are in mixed $Co^{3+/4+}$ states and with increasing Fe ions on Co site Co^{4+} concentration increases. Whereas Fe ions are in $Fe^{2+/3+}$ state and Fe^{2+} state is dominating. The observed magnetic nature is explained by famous Goodenough–Kanamori rule of superexchange. It is concluded that antiferro/ferromagnetic competition is responsible for observed magnetic behavior.

ACKNOWLEDGMENTS

The authors would like to thank DNPL Professor R. C. Budhani for his constant support and encouragement. One of the authors, S. Kumar would like to acknowledge CSIR, India for providing fellowships. V. P. S. Awana is also thankful to Professor E. Takayama Muromauchi for his visit to NIMS, Japan and to carry out the magnetization measurements.

[1]R. Gagnon, C. Lupien, and L. Taillefer, Phys. Rev. B **50**, 3458 (1994).
[2]M. Karppinen, V. P. S. Awana, Y. Morita, and H. Yamauchi, Physica B **312–313**, 62 (2003).
[3]P. R. Slater and C. Greaves, Physica C **180**, 299 (1991).
[4]G. Roth, P. Adelmann, G. Heger, R. Knitter, and T. Wolf, J. Phys. (Paris) **1**, 721 (1991).
[5]Q. Huang, R. J. Cava, A. Santoro, J. J. Krajewski, and W. F. Peck, Physica C **193**, 196 (1992).
[6]T. Krekels, O. Milat, G. Van Tendeloo, S. Amelinckx, T. G. N. Babu, A. J. Wright, and C. Greaves, J. Solid State Chem. **105**, 313 (1993).
[7]J. Ramírez-Castellanos, Y. Matsui, E. Takayama-Muromachi, and M. Isobe, J. Solid State Chem. **123**, 378 (1996).
[8]J. Ramírez-Castellanos, Y. Matsui, M. Isobe, and E. Takayama-Muromachi, J. Solid State Chem. **133**, 434 (1997).
[9]T. Nagai, V. P. S. Awana, E. Takayama-Muromachi, A. Yamazaki, M. Karppinen, H. Yamauchi, S. K. Malik, W. B. Yelon, and Y. Matsuia, J. Solid State Chem. **176**, 213 (2003).
[10]T. Mochiku, Y. Hata, K. Iwase, M. Yonemura, S. Harjo, A. Hoshikawa, K. Oikawa, T. Ishigaki, T. Kamiyama, H. Fujii, F. Izumi, K. Kadowaki, and K. Hirata, Physica B **385–386**, 561 (2006).
[11]P. Zolliker, D. E. Cox, J. M. Tranquada, and G. Shirane, Phys. Rev. B **38**, 6575 (1988)
[12]N. N. Loshkareva, E. A. Gan'shina, B. I. Belevtsev, Y. P. Sukhorukov, E. V. Mostovshchikova, A. N. Vinogradov, V. B. Krasovitsky, and I. N. Chukanova, Phys. Rev. B **68**, 024413 (2003).
[13]S. Yamaguchi, Y. Okimoto, and Y. Tokura, Phys. Rev. B **55**, R8666 (1997).
[14]D. Louca, J. L. Sarrao, J. D. Thompson, H. Roder, and G. H. Kwei, Phys. Rev. B **60**, 10378 (1999).
[15]Y. Kobayashi, N. Fujiwara, S. Murata, K. Asai, and H. Yasuoka, Phys. Rev. B **62**, 410 (2000).
[16]M. A. Korotin, S. Y. Ezhov, I. V. Solovyey, V. I. Anisimov, D. I. Khomskii, and G. A. Sawatzky, Phys. Rev. B **54**, 5309 (1996).
[17]I. Solovyev, N. Hamada, and K. Terakura, Phys. Rev. B **53**, 7158 (1996).
[18]M. Zhuang, W. Zhang, and N. Ming, Phys. Rev. B **57**, 10705 (1997).
[19]J. B. Goodenough, Phys. Rev. **100**, 564 (1955).
[20]J. Kanamori, J. Phys. Chem. Solids **10**, 87 (1959).
[21]J. B. Goodenough, *Magnetism and Chemical Bonds* (Wiley, New York, 1963), pp. 174–178.
[22]R. D. Shannon, Acta Crystallogr., Sect. A: Cryst. Phys., Diffr., Theor. Gen. Crystallogr. **A32**, 751 (1976).
[23]X. G. Luo, X. H. Chen, X. Liu, R. T. Wang, Y. M. Xiong, C. H. Wang, and G. Y. Wang, Phys. Rev. B **70**, 054520 (2004).
[24]T. Mochiku, Y. Mihara, Y. Hata, S. Kamisawa, M. Furuyama, J. Suzuki, K. Kadowaki, N. Metoki, H. Fujii, and K. Hirata, J. Phys. Soc. Jpn. **71**, 790 (2002).
[25]J. C. Dupin, D. Gonbeau, H. Benqlilou-Moudden, Ph. Vinatier, and A. Levasseur, Thin Solid Films **384**, 23 (2001).
[26]T. Fujii, F. M. F. de Groot, G. A. Sawatzky, F. C. Voogt, T. Hibma, and K. Okada, Phys. Rev. B **59**, 3195 (1999).
[27]V. P. S. Awana, S. K. Malik, W. B. Yelon, M. Karppinen, and H. Yanauchi, Physica C **378–381**, 155 (2002).
[28]F. Maury, I. Mirebeau, J. A. Hodges, P. Bourges, Y. Sidis, and A. Forget, Phys. Rev. B **69**, 094506 (2004).
[29]X. Luo, W. Xing, Z. Li, G. Wu, and X. Chen, Phys. Rev. B **75**, 054413 (2007).
[30]J. Wang, Z. D. Wang, W. Zhang, and D. Y. Xing, Phys. Rev. B **66**, 064406 (2002).